ChemComm

COMMUNICATION

View Article Online
View Journal | View Issue

Cite this: *Chem. Commun.*, 2026, **62**, 2672

Received 29th November 2025,
Accepted 5th January 2026

DOI: 10.1039/d5cc06794d

rsc.li/chemcomm

Interphasic separation of *cis*/*trans* perylene-based nanographene isomers driven by selective encapsulation in a supramolecular cage

Carles Fuertes-Espinosa,* Clara Sabrià, Judith Sala, Lorena Capdevila, Ferran Feixas and Xavi Ribas *

The present work describes a supramolecular strategy for the molecular recognition and selective separation of extended PAHs and NGs from isomeric mixtures. This approach consists of a biphasic protocol featuring the selective shuttling of a targeted NG isomer from the organic to the aqueous phase, driven by host–guest interactions with a tetragonal prismatic metal–organic cage (MOC) present in the aqueous layer, while the cage remains permanently confined to the aqueous phase, operating as a static supramolecular receptor throughout the separation process.

Polycyclic aromatic hydrocarbons (PAHs) and nanographenes (NGs) have attracted significant attention in materials science and supramolecular chemistry owing to their distinctive self-assembly[1–3] and optoelectronic properties.[4,5] Their extended π-conjugated frameworks render them promising candidates for advanced functional materials.[6] However, their selective manipulation and separation remain challenging due to strong aggregation, limited solubility, and the structural similarity of related species.[7,8] In particular, the isolation of isomerically pure NGs is challenging, as conventional chromatographic methods are typically solvent-intensive, operationally demanding, and often fail to deliver isomerically pure NG fractions.[9]

In parallel, metal–organic cages (MOCs) have emerged as highly versatile supramolecular platforms, assembled from metal ions and organic ligands, featuring well-defined and tunable cavities.[10–13] Their capacity to trap guest molecules within their confined spaces has been exploited in a broad range of applications, including molecular recognition and purification,[14,15] catalysis,[16] sensing,[17] stabilization of reactive intermediates,[18] and selective molecular transport.[19] The nature of MOC cavities makes them particularly attractive for the recognition of hydrophobic π-conjugated molecules in their confined environments, such as PAHs and fullerenes.[20] However, the confinement of NGs within artificial receptors remains challenging.[21] Supramolecular strategies that exploit host–guest chemistry for molecular separation are gaining increasing interest.[22,23] Recent work by Nitschke and co-workers has shown that phase-transfer of MOCs and their cargoes can be harnessed for practical separation of PAHs.[19,24,25] This approach requires repeated *in situ* anion-exchange steps during the separation cycle, which can lead to the accumulation of salt residues and a progressive decrease in phase-transfer efficiency.[25]

Our previously reported tetragonal prismatic **4**·$(BArF)_8$ cage (Fig. 1a) exhibits strong affinity toward large π-conjugated guests, including fullerenes,[26] endohedral metallofullerenes (EMFs),[27] and fullertubes.[28] The extended planar π-systems of the porphyrin residues in **4**·$(BArF)_8$ and PAHs, suggest the potential for favourable π–π stacking interactions. Hence, we hypothesized that **4**·$(BArF)_8$ would also serve as a suitable host for extended PAHs and NGs.

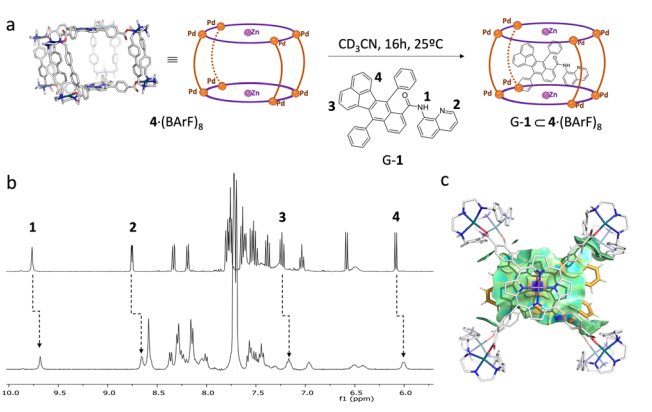

Fig. 1 (a) Schematic representation of the binding of G-**1** within cage **4**·$(BArF)_8$. (b) Stacked partial ^{1}H NMR spectra of G-**1** (top) and G-**1**⊂**4**·$(BArF)_8$ (bottom), showing spectral changes upon host–guest complexation. (c) Representation of non-covalent interaction (NCI) surface of encapsulated G-**1** within the cage (weak van der Waals interactions in green and stronger interactions in blue).

Institut de Química Computacional i Catàlisi (IQCC) and Departament de Química, Universitat de Girona, Girona, 17003, Catalonia, Spain. E-mail: xavi.ribas@udg.edu

Herein, we present a supramolecular strategy for the molecular recognition of extended PAHs and the purification of a perylene-based NGs from a *cis–trans* isomeric mixture. The method exploits selective phase-transfer driven by host–guest interactions, enabling the targeted isomer to shuttle between immiscible solvents. Specifically, a biphasic system was employed in which a mixture of NG isomers was dissolved in the organic phase, while the anionic cage **4**·$(SO_4)_4$ remained in the aqueous phase. This static-host biphasic protocol constitutes an operationally simplified alternative to phase-transfer strategies based on anion-driven cage migration, as it eliminates repeated anion-metathesis events during the separation cycle and enables selective isomer separation through a single, operationally simple biphasic extraction.

G-**1** and G-**2** fluoranthene derivatives, and G-**3**, a *cis-trans* mixture of perylene-based NG, were synthesized and characterized following protocols previously reported by our group.[29] The selected nanographenes serve as representative scaffolds of structurally sophisticated and elaborated NGs, allowing the evaluation of the **4**·$(BArF)_8$ capacity to selectively separate *cis*/*trans* isomeric mixtures.

To study the molecular recognition of G-**1** within the tetragonal prismatic cage **4**·$(BArF)_8$, a stoichiometric amount of G-**1** (Fig. S1–S3) stock solution was added into a solution of the host in CD_3CN (Fig. 1a).

The host–guest complex G-**1**⊂**4**·$(BArF)_8$ was characterized by ^{1}H NMR (Fig. 1b and Fig. S4), high-resolution mass spectrometry (HRMS) (Fig. S5) and NOESY NMR (Fig. S6). In the ^{1}H NMR spectrum, the signals of G-**1** underwent upfield shifts attributed to the inclusion-induced shielding effect (Fig. 1b and Fig. S4), consistent with guest encapsulation within the cavity of **4**·$(BArF)_8$ in a fast-exchange regime at the NMR timescale. Binding was further evidenced by broadening of the G-**1** proton signals (Fig. 1b and Fig. S4 and S7). Concomitant shifts and broadening of the signals of the protons of the metalloporphyrin residues of the cage, together with the NOESY correlations observed, indicated participation of these π-conjugated panels in the guest binding (Fig. S4, S6, S7 and S8). ^{1}H DOSY NMR spectrum showed that host–guest signals present similar diffusion coefficients to free **4**·$(BArF)_8$, suggesting the formation of an inclusion complex (Fig. S10). Furthermore, as the G-**1**⊂**4**·$(BArF)_8$ adduct equilibrated in fast exchange on the NMR timescale, ^{1}H DOSY NMR analysis of the encapsulated G-**1** signals afforded a diffusion coefficient larger than the free G-**1**, providing further evidence of the formation of a host–guest adduct (Fig. S11). ^{1}H NMR titration experiments provide an association constant K_a = 4.03 (±0.1) × 10^4 M^{-1} for the formation of G-**1**⊂**4**·$(BArF)_8$ (Fig. S11). Mole-ratio analysis (Fig. S12) supported the formation of a 1 : 1 host–guest complex and ESI-HRMS (Fig. S5) corroborated the stoichiometry, revealing distinct $[G\text{-}\mathbf{1}\subset\mathbf{4}]^{n+}$ peaks.

The molecular recognition of G-**2** (Fig. S20a), featuring an ethylene bridge on the fluoranthene unit (Fig. S13–S15), was investigated using an analogous protocol to that employed for G-**1**. An equimolar mixture of **4**·$(BArF)_8$ and G-**2** results in the corresponding 1 : 1 host–guest complex, as confirmed by mole-ratio analysis (Fig. S16) and ESI-HRMS (Fig. S17). The ^{1}H NMR signals of the porphyrin protons in **4**·$(BArF)_8$ broadened and shifted upfield, consistent with altered cage symmetry upon encapsulation of G-**2** (Fig. S19 and S20b). Simultaneously, the guest signals exhibited upfield shifts characteristic of an inclusion complex, indicating fast-exchange binding on the NMR timescale (Fig. S20). Notably, the differences in NMR response between G-**2** and G-**1** were attributed to changes in cage symmetry rather than binding stoichiometry. NOESY correlations indicated participation of the π-conjugated panels of G-**2** and the porphyrin residues of the cage in the binding event (Fig. S18). ^{1}H NMR titration experiments revealed an association constant K_a = 5.41 (± 0.1) × 10^4 M^{-1} (Fig. S21), slightly higher than to that observed for G-**1**. Moreover, the diffusion experiments resulted in a diffusion coefficient for the confined G-**2** larger than for free G-**2** guest, providing further evidence on the formation of G-**2**⊂**4**·$(BArF)_8$ host–guest complex (Fig. S22). To get further insight into the non-covalent interactions directing the molecular recognition of G-**1** and G-**2**, molecular dynamics (MD) simulations for G-**1**⊂**4**·Cl_8 and G-**2**⊂**4**·Cl_8 host–guest adducts were carried out (Fig. 1c and Fig. S23 and S24). In both cases, a persistent interaction between the oxygen of the carbonyl group of the guests and the Zn atom on the porphyrin of the cage was identified (Fig. S23). The noncovalent interaction (NCI) volumes were also calculated for both systems,[30] observing a slightly larger value for G-**2** (971.3 ± 78.4 Å^3) than for G-**1** (901.0 ± 79.1 Å^3) (Fig. 1c and Fig. S24). This indicates higher stabilization of the host–guest adduct, which can be correlated with higher affinity of the host towards G-**2**. The enhanced binding of G-**2** compared to G-**1** could be tentatively assigned to additional aliphatic CH_2–π interactions between the ethylene bridge of G-**2** and the aromatic panels of the host cavity (Fig. S25), which could act cooperatively with the dominant π–π interactions.

Given the effective encapsulation of G-**1** and G-**2**, we envisioned that **4**·$(BArF)_8$ could host extended perylene-based NGs guests, such as *cis*/*trans*-G-**3** isomeric mixture (Fig. 2a and Fig. S26 and S27). Upon adding an equimolar amount of *cis*/*trans*-G-**3** into a CD_3CN solution of **4**·$(BArF)_8$, the chemical shifts of the signals of the host and guest's protons showed marked changes, with some of the peaks undergoing severe broadening (Fig. S28). These observations in the ^{1}H NMR spectrum indicated the formation of a host–guest complex. However, the broadening of the peaks of the *cis*/*trans*-G-**3** isomeric mixture in the ^{1}H NMR (Fig. S29) precluded its identification when confined (attempts to assign the confined guest signals based on variable temperature ^{1}H NMR, 2D ^{1}H–^{1}H COSY, and NOESY were unsuccessful). Encapsulation/dissociation of the *cis*/*trans*-G-**3**⊂**4**·$(BArF)_8$ occurs under fast exchange at the NMR time scale, given that signals of the host (in the host–guest adduct) are shifted and broadened; however, a new set of signals corresponding to the encapsulated guest was not observed (Fig. S28 and S29). Stoichiometric analysis (Fig. S30b) indicated the formation of a 1 : 1 inclusion complex. To further confirm the confinement of the NGs mixture, the formation of the *cis*/*trans*-G-**3**⊂**4**·$(BArF)_8$ complex was studied by ESI-HRMS

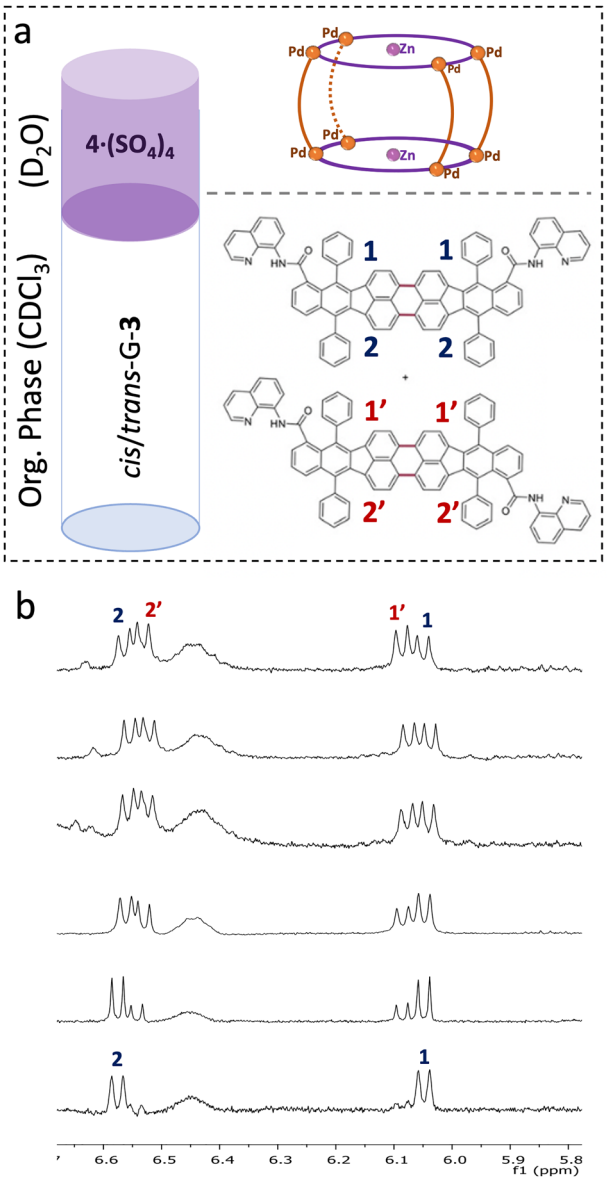

Fig. 2 (a) Schematic representation of the biphasic system designed to purify *cis*/*trans*-G-**3** NGs. (b) Stacked partial ^{1}H NMR spectra of *cis*/*trans*-G-**3** isomeric mixture, showing spectral changes upon selective host–guest complexation of *trans*-G-**3** along the time (15 min intervals; time = 0, top spectrum; time = 75 minutes, bottom spectrum).

(Fig. S30a), revealing distinct [*cis*/*trans*-G-**3**⊂**4**]$^{n+}$ peaks with a 1 : 1 binding ratio. To quantify the binding of **4**·(BArF)$_8$ towards *cis*/*trans*-G-**3** mixture, an inverse titration was carried out; the signals attributed to the guest were monitored by ^{1}H NMR upon the sequential addition of a stock solution of the host (Fig. S31). The titration resulted in an association constant K_a = 1.32 (± 0.1) × 10^5 M^{-1}.

Since conventional chromatographic and crystallization methods lacked sufficient selectivity to separate the *cis*-G-**3** and *trans*-G-**3** isomers, and both *cis* and *trans* isomers of G-**3** showed host–guest interactions with **4**·(BArF)$_8$ in homogeneous solutions (Fig. S31.a), we designed a biphasic protocol to attempt their separation. Many organic guests are soluble in a wide range of water-immiscible organic solvents, making the water/organic system the most versatile setup. Water-soluble cage **4**·(SO$_4$)$_4$ was synthesized following previously reported protocols,[31] utilizing as a precursor **4**·(BArF)$_8$. We evaluated the selectivity of **4**·(SO$_4$)$_4$ towards the *cis*- and *trans*-G-**3** isomers using a biphasic system composed of D$_2$O, containing **4**·(SO$_4$)$_4$ (one equivalent per equivalent of *trans*-G-**3**), and CDCl$_3$ as the organic layer containing a mixture of *cis*/*trans*-G-**3** isomers (Fig. 2a). Previous studies suggested that the host–guest properties of **4**·(BArF)$_8$ are not strongly affected by the counteranion present in the cage structure.[26,31] The organic phase was monitored by ^{1}H NMR over 75 minutes. The spectra revealed a pronounced change in the isomeric ratio—from an initial 40 : 60 (*cis* : *trans*) composition to 95 : 5 after 75 minutes—indicating preferential transfer of the *trans*-G-**3** isomer (Fig. 2b) into the aqueous phase. ^{1}H NMR quantification (using mesitylene as an internal standard) of the *trans*-G-**3**, indicated that ∼90% of this isomer migrated from the CDCl$_3$ phase into the D$_2$O phase (Fig. 2b). Upon acid treatment of the aqueous phase, the cage was disassembled and the *trans*-G-**3** released (after acid-mediated disassembly, the cage can be reassembled and recovered by basification (∼80%)).[32] The ^{1}H NMR spectrum of the released guest revealed >90% of *trans*-G-**3** (Fig. S32), showing only trace amounts of *cis*-G-**3**. These results indicate higher affinity of **4**·(SO$_4$)$_4$ towards *trans*-G-**3**, enabling its selective shuttling into the aqueous phase through host–guest encapsulation within the interphase of the biphasic system. Notably, this purification process does not require cage transfer reactions nor external manipulation, offering a more practical and potentially scalable alternative to conventional phase-transfer purification methods. Conventional chromatographic methods fail to isolate pure *trans*-G-**3** isomer, due to their nearly identical π-surfaces and polarity. This highlights the operational advantage of the biphasic extraction.

The two isomers (*cis*- and *trans*-) of G-**3** and their corresponding host–guest complexes were studied by MD simulations (Fig. 3). In the MD simulations corresponding to *trans*-G-**3** ⊂ **4**·Cl$_8$, the guest is completely confined within the cage cavity with extensive interactions of the perylene unit with the Zn–porphyrin of the cage (Fig. 3b and Fig. S33). In contrast, for the *cis*-G-**3** ⊂ **4**·Cl$_8$, the guest is not completely confined within the cage along all the MD simulation, being sterically excluded from the centre of the cavity, and it is found interacting on the periphery of one of the four cage windows (Fig. 3b and Fig. S33). This suggests that having the 8-aminoquinoline substituents on the same side (as in the *cis* isomer) makes the NG unable to fit inside the cavity of the host due to steric clashes with the macrocycles of the host. Contrariwise, having the 8-aminoquinoline substituents on different sides (as in the *trans* isomer) the NG can fit perfectly inside the confined cavity of the cage. The NCI volumes indicated pronounced interactions for the *trans* isomer, due to the perylene unit interacting with the Zn–porphyrin (1700.8 ± 141.4 Å^3 for the *trans*-G-**3**), while much weaker interactions for the *cis*-isomer (971.3 ± 78.4 Å^3 for the *cis*-G-**3**) (Fig. 3b and Fig. S33), in agreement with the

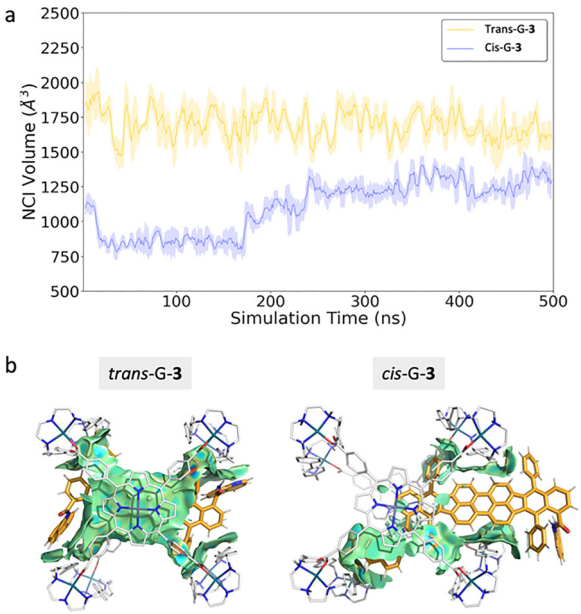

Fig. 3 (a) Calculated NCI volumes *versus* the simulation time along one replicate for isomers *cis*- and *trans*-G-**3** inside the cage. (b) Representation of NCI surface of each encapsulated nanographene with the cage (weak van der Waals interactions in green and stronger interactions in blue).

experimental results. Of note, the neat *cis*/*trans*-G-**3** separation is only achieved upon biphasic phase-to-phase-transfer, whereas no separation is observed in a single-phase encapsulation.

^{1}H NMR titration tests with three commercial PAHs (coronene, pyrene, perylene) show measurable weak binding only for perylene (Fig. S34). Extended perylene derivatives (such as *cis*/*trans*-G-**3**) show better matching with the cage cavity size, exhibiting stronger binding towards **4**·$(BArF)_8$. These observations emphasize the importance of the size complementarity between the host and guest for the efficient recognition of NGs.

In summary, we have developed a supramolecular strategy for the selective recognition and phase-transfer purification of extended perylene-based NGs using a tetragonal prismatic MOC. The water-soluble anionic cage **4**·$(SO_4)_4$ enables the selective shuttling of the *trans*-G-**3** isomer from the organic to the aqueous phase through host–guest interactions operating at the liquid–liquid interface, without requiring cage migration, anion metathesis, or external manipulation. This process achieves efficient isomeric discrimination—transferring over 90% of the *trans* isomer into the aqueous phase—while avoiding the generation of salt by-products associated with conventional phase-transfer protocols. NMR, HRMS, and MD simulations studies reveal that the *trans*-G-**3** isomer fits fully within the cage cavity through non-covalent interactions with the Zn–porphyrin residues, whereas the *cis* isomer is sterically excluded. By circumventing repeated cage migration steps and enabling autonomous, selective phase-transfer of the targeted guest, this strategy represents a significant step toward practical and scalable supramolecular separation processes, bridging the gap between fundamental host–guest chemistry and industrial molecular purification.

This work was supported by MCIN Spain (PID2022-136970NB-I00 and TED2021-130573B-I00 to X.R., RYC2020-029552-I, and PID2022-141676NB-I00 to F. F.) and Generalitat de Catalunya (2021SGR00475, 2021SGR00487). C. F. and J. S. thank GenCat for a BdP and FI grant, respectively. C. S. thanks UdG for a PhD grant. X. R. is also grateful for an ICREA-Academia award.

Conflicts of interest

There are no conflicts to declare.

Data availability

The data supporting this article have been included as part of supplementary information (SI). Supplementary information includes synthesis protocols, spectroscopic characterization, and MD studies. See DOI: https://doi.org/10.1039/d5cc06794d.

References

1 J. Wu, W. Pisula and K. Müllen, *Chem. Rev.*, 2007, **107**, 718–747.
2 A. Narita, X.-Y. Wang, X. Feng and K. Müllen, *Chem. Soc. Rev.*, 2015, **44**, 6616–6643.
3 I. Matsumoto, R. Sekiya and T. Haino, *Angew. Chem., Int. Ed.*, 2021, **60**, 12706–12711.
4 Y. Gu, Z. Qiu and K. Müllen, *J. Am. Chem. Soc.*, 2022, **144**, 11499–11524.
5 Z. Qiu, C.-W. Ju, L. Frédéric, Y. Hu, D. Schollmeyer, G. Pieters, K. Müllen and A. Narita, *J. Am. Chem. Soc.*, 2021, **143**, 4661–4667.
6 M. Buendía, J. M. Fernández-García, J. Perles, S. Filippone and N. Martín, *Nat. Synth.*, 2024, **3**, 545–553.
7 D. Reger, P. Haines, F. W. Heinemann, D. M. Guldi and N. Jux, *Angew. Chem., Int. Ed.*, 2018, **57**, 5938–5942.
8 X.-H. Ma, X. Gao, J.-Y. Chen, M. Cao, Q. Dai, Z.-K. Jia, Y.-B. Zhou, X.-J. Zhao, C. Chu, G. Liu and Y.-Z. Tan, *J. Am. Chem. Soc.*, 2024, **146**, 2411–2418.
9 V. Kumar, J. L. Páez, S. Míguez-Lago, J. M. Cuerva, C. M. Cruz and A. G. Campaña, *Chem. Soc. Rev.*, 2025, **54**, 4922–4947.
10 C. J. T. Cox, J. Hale, P. Molinska and J. E. M. Lewis, *Chem. Soc. Rev.*, 2024, **53**, 10380–10408.
11 T. Tozawa, J. T. A. Jones, S. I. Swamy, S. Jiang, D. J. Adams, S. Shakespeare, R. Clowes, D. Bradshaw, T. Hasell, S. Y. Chong, C. Tang, S. Thompson, J. Parker, A. Trewin, J. Bacsa, A. M. Z. Slawin, A. Steiner and A. I. Cooper, *Nat. Mater.*, 2009, **8**, 973–978.
12 M. Yoshizawa, J. K. Klosterman and M. Fujita, *Angew. Chem., Int. Ed.*, 2009, **48**, 3418–3438.
13 R. Chakrabarty, P. S. Mukherjee and P. J. Stang, *Chem. Rev.*, 2011, **111**, 6810–6918.
14 D. Zhang, T. K. Ronson, Y.-Q. Zou and J. R. Nitschke, *Nat. Rev. Chem.*, 2021, **5**, 168–182.
15 L.-J. Chen, H.-B. Yang and M. Shionoya, *Chem. Soc. Rev.*, 2017, **46**, 2555–2576.
16 M. Morimoto, S. M. Bierschenk, K. T. Xia, R. G. Bergman, K. N. Raymond and F. D. Toste, *Nat. Catal.*, 2020, **3**, 969–984.
17 Y. Zhou, H. Li, T. Zhu, T. Gao and P. Yan, *J. Am. Chem. Soc.*, 2019, **141**, 19634–19643.
18 A. Galan and P. Ballester, *Chem. Soc. Rev.*, 2016, **45**, 1720–1737.
19 D. Zhang, T. K. Ronson, R. Lavendomme and J. R. Nitschke, *J. Am. Chem. Soc.*, 2019, **141**, 18949–18953.
20 F. J. Rizzuto, L. K. S. von Krbek and J. R. Nitschke, *Nat. Rev. Chem.*, 2019, **3**, 204–222.
21 H. Wu, Y. Wang, B. Song, H.-J. Wang, J. Zhou, Y. Sun, L. O. Jones, W. Liu, L. Zhang, X. Zhang, K. Cai, X.-Y. Chen, C. L. Stern, J. Wei, O. K. Farha, J. M. Anna, G. C. Schatz, Y. Liu and J. Fraser Stoddart, *Nat. Commun.*, 2021, **12**, 5191.

22 S. La Cognata and V. Amendola, *Chem. Commun.*, 2023, **59**, 13668–13678.
23 Y.-L. Lu, Y.-P. Wang, K. Wu, M. Pan and C.-Y. Su, *Acc. Chem. Res.*, 2024, **57**, 3277–3291.
24 A. B. Grommet and J. R. Nitschke, *J. Am. Chem. Soc.*, 2017, **139**, 2176–2179.
25 A. B. Grommet, J. B. Hoffman, E. G. Percástegui, J. Mosquera, D. J. Howe, J. L. Bolliger and J. R. Nitschke, *J. Am. Chem. Soc.*, 2018, **140**, 14770–14776.
26 C. García-Simón, M. Garcia-Borràs, L. Gómez, T. Parella, S. Osuna, J. Juanhuix, I. Imaz, D. Maspoch, M. Costas and X. Ribas, *Nat. Commun.*, 2014, **5**, 5557.
27 C. Fuertes-Espinosa, A. Gómez-Torres, R. Morales-Martínez, A. Rodríguez-Fortea, C. García-Simón, F. Gándara, I. Imaz, J. Juanhuix, D. Maspoch, J. M. Poblet, L. Echegoyen and X. Ribas, *Angew. Chem., Int. Ed.*, 2018, **57**, 11294–11299.
28 V. Iannace, C. Sabrià, R. D. Schmitt, F. Feixas, S. Stevenson and X. Ribas, *J. Am. Chem. Soc.*, 2025, **147**, 36079–36084.
29 L. Capdevila, J. Sala, C. Berga, A. de Aquino, T. Parella, L. Blancafort, L. Rodríguez, S. Simon and X. Ribas, *ChemistryEurope*, 2025, **3**, e202500102.
30 R. A. Boto, F. Peccati, R. Laplaza, C. Quan, A. Carbone, J.-P. Piquemal, Y. Maday and J. Contreras-García, *J. Chem. Theo. Comput.*, 2020, **16**, 4150–4158.
31 C. Fuertes-Espinosa, C. García-Simón, M. Pujals, M. Garcia-Borràs, L. Gómez, T. Parella, J. Juanhuix, I. Imaz, D. Maspoch, M. Costas and X. Ribas, *Chem*, 2020, **6**, 169–186.
32 C. Colomban, C. Fuertes-Espinosa, S. Goeb, M. Sallé, M. Costas, L. Blancafort and X. Ribas, *Chem. – Eur. J.*, 2018, **24**, 4371–4381.

